

## Research Article

# E22 $\Delta$ Mutation in Amyloid $\beta$ -Protein Promotes $\beta$ -Sheet Transformation, Radical Production, and Synaptotoxicity, But Not Neurotoxicity

Takayuki Suzuki,<sup>1</sup> Kazuma Murakami,<sup>1</sup> Naotaka Izuo,<sup>2</sup> Toshiaki Kume,<sup>2</sup> Akinori Akaike,<sup>2</sup> Tetsu Nagata,<sup>3</sup> Tomoyuki Nishizaki,<sup>3</sup> Takami Tomiyama,<sup>4</sup> Hiroshi Takuma,<sup>4</sup> Hiroshi Mori,<sup>4</sup> and Kazuhiro Irie<sup>1</sup>

<sup>1</sup>Laboratory of Organic Chemistry in Life Science, Division of Food Science and Biotechnology, Graduate School of Agriculture, Kyoto University, Sakyo-ku, Kyoto 606-8502, Japan

<sup>2</sup>Department of Pharmacology, Graduate School of Pharmaceutical Sciences, Kyoto University, Sakyo-ku, Kyoto 606-8501, Japan

<sup>3</sup>Department of Physiology, Hyogo College of Medicine, Nishinomiya 663-8501, Japan

<sup>4</sup>Department of Neuroscience, Graduate School of Medicine, Osaka City University, Osaka 545-8585, Japan

Correspondence should be addressed to Kazuhiro Irie, irie@kais.kyoto-u.ac.jp

Received 16 October 2010; Accepted 16 November 2010

Academic Editor: Katsuhiko Yanagisawa

Copyright © 2011 Takayuki Suzuki et al. This is an open access article distributed under the Creative Commons Attribution License, which permits unrestricted use, distribution, and reproduction in any medium, provided the original work is properly cited.

Oligomers of 40- or 42-mer amyloid  $\beta$ -protein ( $A\beta_{40}$ ,  $A\beta_{42}$ ) cause cognitive decline and synaptic dysfunction in Alzheimer's disease. We proposed the importance of a turn at Glu22 and Asp23 of  $A\beta_{42}$  to induce its neurotoxicity through the formation of radicals. Recently, a novel deletion mutant at Glu22 (E22 $\Delta$ ) of  $A\beta_{42}$  was reported to accelerate oligomerization and synaptotoxicity. To investigate this mechanism, the effects of the E22 $\Delta$  mutation in  $A\beta_{42}$  and  $A\beta_{40}$  on the transformation of  $\beta$ -sheets, radical production, and neurotoxicity were examined. Both mutants promoted  $\beta$ -sheet transformation and the formation of radicals, while their neurotoxicity was negative. In contrast, E22P- $A\beta_{42}$  with a turn at Glu22 and Asp23 exhibited potent neurotoxicity along with the ability to form radicals and potent synaptotoxicity. These data suggest that conformational change in E22 $\Delta$ - $A\beta$  is similar to that in E22P- $A\beta_{42}$  but not the same, since E22 $\Delta$ - $A\beta_{42}$  exhibited no cytotoxicity, unlike E22P- $A\beta_{42}$  and wild-type  $A\beta_{42}$ .

## 1. Introduction

Alzheimer's disease (AD) is characterized by amyloid deposition in senile plaques that are mainly composed of 40- and 42-mer amyloid  $\beta$ -proteins ( $A\beta_{40}$  and  $A\beta_{42}$ ) [1, 2]. These proteins are secreted from amyloid precursor protein (APP) by two proteases,  $\beta$ - and  $\gamma$ -secretases [3].  $A\beta_{42}$  plays a more critical role in the pathogenesis of AD than  $A\beta_{40}$  because of its stronger aggregative ability and neurotoxicity [3]. Oxidative stress is believed to contribute to neuronal loss in AD [4–6]; one of the proposed mechanisms of  $A\beta_{42}$ -induced neurotoxicity is related to the radicalization at both Tyr10 and Met35 accompanied by the generation of hydrogen peroxide [7, 8]. On the other hand, soluble oligomeric

assembly of  $A\beta$  causes cognitive impairment and synaptic dysfunction in AD [9, 10].

Our previous investigation using solid-state NMR together with systematic proline replacement proposed a toxic conformer with a turn at positions 22 and 23 in  $A\beta_{42}$  aggregates and a nontoxic conformer with a turn at positions 25 and 26; the former showed a potent ability to aggregate, form oligomers, and exhibit neurotoxicity [11]. The turn formation at positions 22 and 23 along with the neighboring  $\beta$ -sheet structure in the toxic conformer of  $A\beta_{42}$  brought Tyr10 and Met35 close together to generate the S-oxidized radical cation at Met35, the ultimate toxic radical species, through oxidation by the phenoxy radical at Tyr10 produced by redox reactions [7, 12]. The mutations of  $A\beta$  are concentrated at

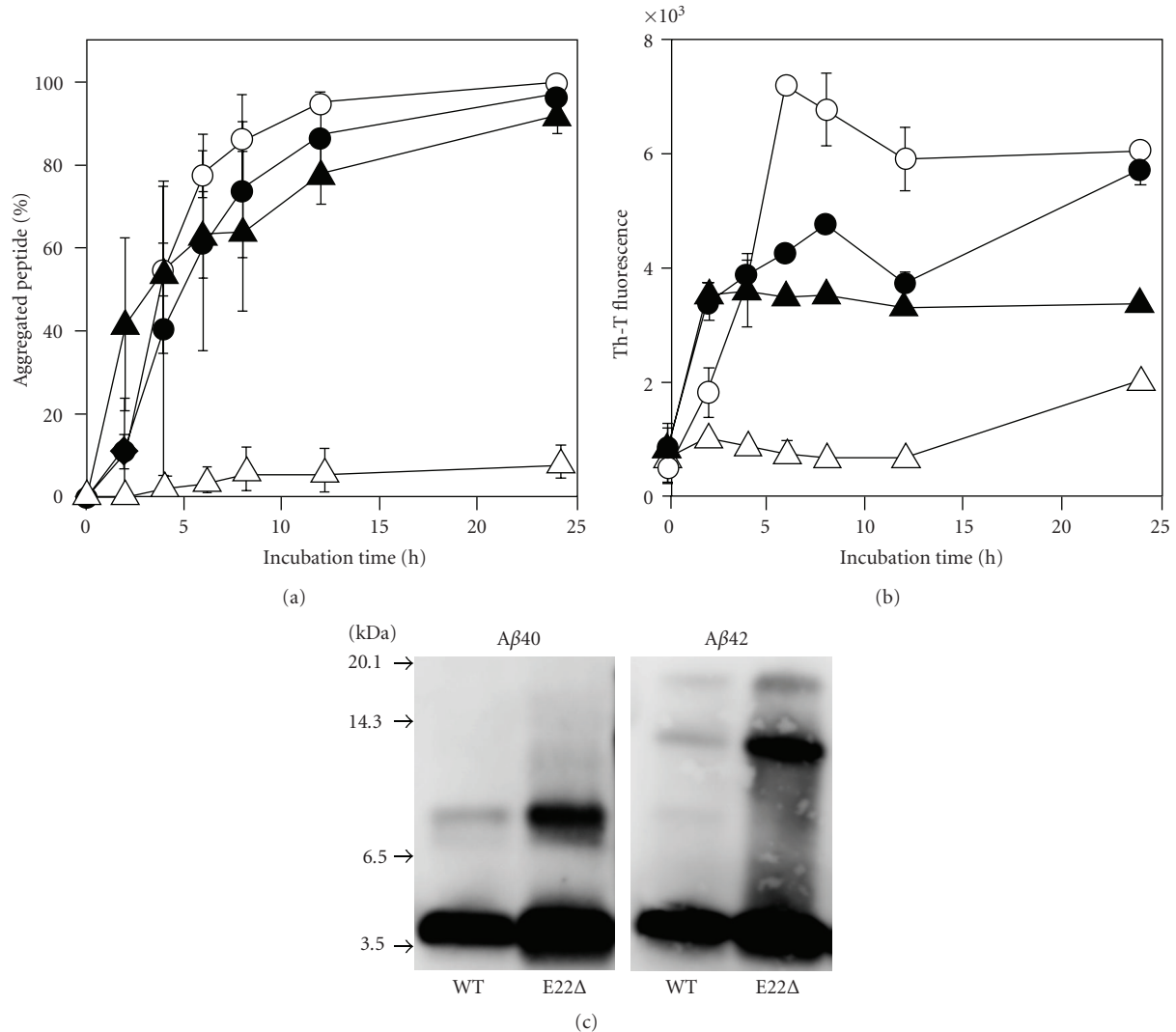


FIGURE 1: Aggregation profiles of E22Δ-Aβ40 and E22Δ-Aβ42 (25 μM) after incubation at 37°C. (a) Sedimentation assay estimated by HPLC analysis after centrifugation. (b) Th-T fluorescence assay. ○, Aβ42; △, Aβ40; ●, E22Δ-Aβ42; ▲, E22Δ-Aβ40. (c) Western blotting without incubation.

positions 21, 22, and 23; A21G (Flemish), E22G (Arctic), E22Q (Dutch), E22K (Italian), and D23N (Iowa) types. These mutations may play a pathological role in cerebral amyloid angiopathy (CAA) or familial AD (FAD) because these mutant proteins induced neuronal death *in vitro* more potently than wild-type Aβ42 [13]. Thus, Glu22 and Asp23 in Aβ are considered to be key residues for neurotoxicity through the formation of radicals.

Recently, Mori and coworkers reported that a novel mutation, in which the Glu-22 residue is defective (E22Δ), induced AD-type dementia without amyloid deposition, and that *in vitro* E22Δ-Aβ42 favorably formed low-molecular weight oligomers to inhibit long-term potentiation (LTP) compared with Aβ42 [14] and to induce synaptic alteration [15]. Therefore, the effects of the deletion at Glu22 on the secondary structure, formation of radicals, and neurotoxicity

are interesting from the standpoint of discussing the role of the Glu-22 residue of Aβ42 in the pathogenesis of AD.

This paper describes a comprehensive study of the aggregative ability, secondary structure, radical-generating activity, neurotoxicity in primary rat cortical neuronal cell cultures, and the inhibitory activity of LTP of both E22Δ-Aβ40 and E22Δ-Aβ42. These results were compared with those of E22P-Aβ42 with a turn at positions 22 and 23.

## 2. Materials and Methods

**2.1. Preparation of E22Δ-Aβ.** E22Δ-Aβ40 and E22Δ-Aβ42 were synthesized by the method reported previously [16]. Their molecular weights were confirmed by matrix-assisted laser desorption/ionization time-of-flight mass spectrometry (MALDI-TOF-MS): E22Δ-Aβ40 (*m/z*: calcd: 4201.76; found:

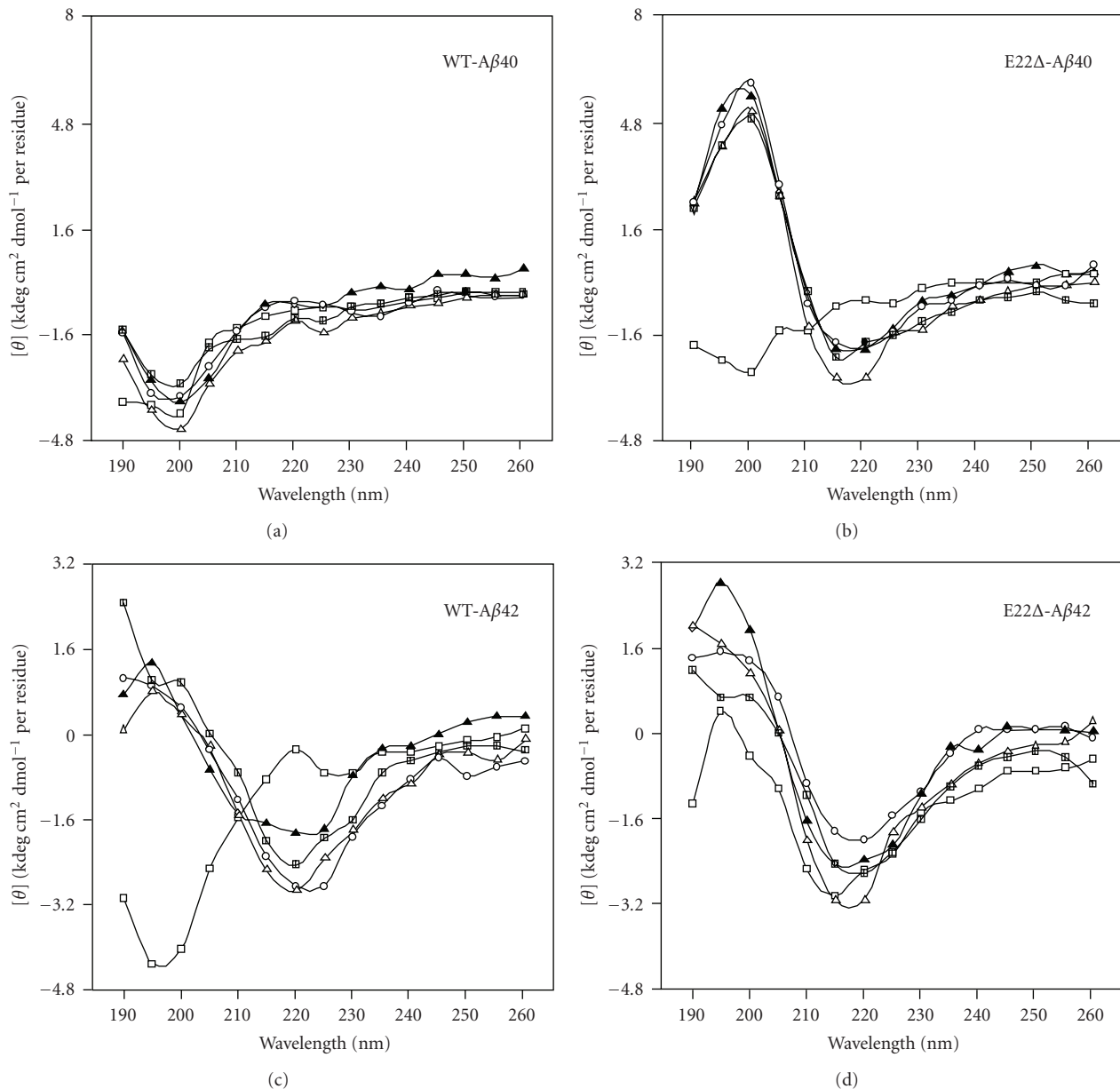


FIGURE 2: CD spectra of E22 $\Delta$ -A $\beta$ 40 and E22 $\Delta$ -A $\beta$ 42 (25  $\mu\text{M}$ ). (a) A $\beta$ 40, (b) E22 $\Delta$ -A $\beta$ 40, (c) A $\beta$ 42, (d) E22 $\Delta$ -A $\beta$ 42. Each A $\beta$  (25  $\mu\text{M}$ ) was incubated in phosphate buffer at 37°C for the following times:  $\square$ , 0 h;  $\blacktriangle$ , 4 h;  $\triangle$ , 8 h;  $\circ$ , 24 h;  $\blacksquare$ , 48 h.

4201.56  $[\text{M} + \text{H}]^+$ , E22 $\Delta$ -A $\beta$ 42 ( $m/z$ : calcd: 4386.00; found: 4385.98  $[\text{M} + \text{H}]^+$ ).

**2.2. Sedimentation Assay.** The aggregation kinetics of each A $\beta$  (25  $\mu\text{M}$ ) was estimated with the sedimentation assay using HPLC. The experimental procedure was described elsewhere [13]. The area of absorption at 220 nm was integrated and expressed as a percentage of the control.

**2.3. Thioflavin T (Th-T) Fluorescence Assay.** Aggregative ability of each A $\beta$  (25  $\mu\text{M}$ ) was evaluated by the Th-T method developed by Naiki and Gejyo [17]. The measurement was performed on a Multidetector Microplate

Reader powerscan HT (Dainippon Sumitomo Pharma) at room temperature, as described elsewhere [13]. Fluorescence intensity was measured at 450 nm excitation and 482 nm emission.

**2.4. Western Blotting.** Gel electrophoresis using 10–20% Tricine gel (Invitrogen, Carlsbad, CA) and Western blots analysis were carried out according to the manufacturer's protocol. The experimental procedure was described elsewhere [12]. Briefly, each A $\beta$  was dissolved in 0.1%  $\text{NH}_4\text{OH}$  at 250  $\mu\text{M}$ . After a 10-fold dilution by 50 mM sodium phosphate containing 100 mM NaCl at pH 7.4, the resultant peptide solution (25  $\mu\text{M}$ ) was incubated for 0, 2, or 4 hr at

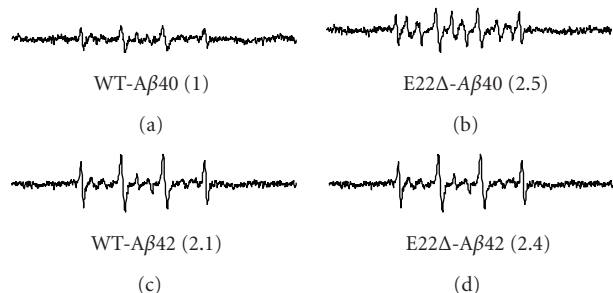


FIGURE 3: ESR spectra of E22 $\Delta$ -A $\beta$ 40 and E22 $\Delta$ -A $\beta$ 42 (100  $\mu$ M) after 48-hr incubation at 37°C. (a) A $\beta$ 40, (b) E22 $\Delta$ -A $\beta$ 40, (c) A $\beta$ 42, (d) E22 $\Delta$ -A $\beta$ 42. The spectra of A $\beta$  are shown after subtraction of the background spectrum in the presence of PBN without A $\beta$ . Numbers in parentheses represent relative integral intensities of ESR signals, where the intensity of A $\beta$ 40 was taken as 1.0.

37°C. The anti-N-terminus of A $\beta$  antibody, 82E1, (Immuno-Biological Laboratories Co., Ltd., Gunma, Japan) was used at 1  $\mu$ g/mL as the primary antibody.

**2.5. CD Spectrometry.** Each A $\beta$  was dissolved in 0.1% NH<sub>4</sub>OH at 250  $\mu$ M and diluted 10 times with 50 mM phosphate buffer (pH 7.12). The procedure was described elsewhere [16].

**2.6. ESR Spectrometry.** A reliable method for estimating the ability of A $\beta$  (100  $\mu$ M) to produce radicals using ESR was developed by Butterfield's group [18]. ESR spectrometry was performed on an EMX ESR spectrometer (Bruker BioSpin K.K., Karlsruhe, Germany) at room temperature, as described elsewhere [19].

**2.7. Estimation of Cell Survival.** To evaluate the neurotoxicity of A $\beta$  using an MTT assay, we used undifferentiated PC12 cells, which have the potential to differentiate into neural cells, are sensitive to A $\beta$ , and are generally used for detecting neurotoxicity as a neurotoxicity model [20]. The experimental procedure was described elsewhere [15].

**2.8. Preparation of Primary Culture and Estimation of Cell Survival.** Near-pure neuronal cultures were obtained from the cerebral cortices of fetal rats (17–19 days of gestation) as described [21, 22]. Cultures were maintained in Eagle's MEM supplemented with 10% heat-inactivated fetal bovine serum or 10% heat-inactivated horse serum at 37°C in a humidified 5% CO<sub>2</sub> atmosphere. To prevent the proliferation of nonneural cells, 10  $\mu$ M cytosine  $\beta$ -arabino-furanoside hydrochloride was added after 5 days of plating. In all experiments mature cells used after 11–13 days *in vitro*. Animals were treated in accordance with the guidelines of the Kyoto University animal experimentation committee and the guidelines of the Japanese Pharmacological Society.

Each A $\beta$  was dissolved in 0.02% NH<sub>4</sub>OH at 200  $\mu$ M and diluted on ice immediately before treatment. After

48 hr treatment, neurotoxicity was evaluated by lactate dehydrogenase (LDH) release assay and MTT assay.

**2.9. Long-Term Potentiation.** Field excitatory postsynaptic potentials (fEPSPs) were recorded from the CA1 region of rat hippocampal slices (Wistar rats, male, 6 weeks old) by electrically stimulating the Schaffer collateral [23]. Hippocampal slices were soaked in E22 $\Delta$ -A $\beta$ 40, E22 $\Delta$ -A $\beta$ 42, and E22P-A $\beta$ 42 solution [20  $\mu$ g/200 mL phosphate-buffered saline (PBS)] before high-frequency stimulation (5 trains consisted of four 100-Hz pulses with an intertrain interval of 200 ms). fEPSPs were measured in the presence and absence of each A $\beta$ .

### 3. Results and Discussion

**3.1. Aggregative Ability of E22 $\Delta$  Mutants.** E22 $\Delta$ -A $\beta$ 40 and E22 $\Delta$ -A $\beta$ 42 were examined for their aggregative ability by a sedimentation assay: HPLC analysis after centrifugation of each A $\beta$  solution. Both E22 $\Delta$ -A $\beta$ 40 and E22 $\Delta$ -A $\beta$ 42 aggregated at a velocity similar to A $\beta$ 42, while A $\beta$ 40 hardly aggregated even after 24-hr incubation (Figure 1(a)). This suggests that the ability to form aggregates of both E22 $\Delta$ -A $\beta$ 40 and E22 $\Delta$ -A $\beta$ 42 would be comparable to that of A $\beta$ 42 though soluble A $\beta$  assemblies (oligomers) could not be distinguished from high-molecular weight fibrils in this assay condition (centrifugation: 20,000 g  $\times$  10 min). In the Th-T assay, which can estimate the  $\beta$ -sheet structure in A $\beta$  aggregates [17], E22 $\Delta$ -A $\beta$ 40 showed higher fluorescence than A $\beta$ 40. In contrast, the maximum fluorescence of E22 $\Delta$ -A $\beta$ 42 did not exceed that of A $\beta$ 42, although the velocity of E22 $\Delta$ -A $\beta$ 42 showing fluorescence was slightly higher than that of A $\beta$ 42 (Figure 1(b)). These data suggest that the E22 $\Delta$  mutation accelerates the aggregation of A $\beta$ .

Western blotting was carried out to estimate accurately the oligomerization state of A $\beta$ . E22 $\Delta$ -A $\beta$ 42 formed trimers exclusively, but E22 $\Delta$ -A $\beta$ 40 produced dimers immediately after incubation (Figure 1(c)), as did the cases in the paper by Tomiyama et al. [14]; however, our Th-T assay results do not coincide with their results [14]; under Tomiyama's conditions, both mutants showed almost no fluorescence, even after 7 days. This discrepancy of the Th-T test may be due to the different conditions to make aggregates, presumably resulting in the generation of oligomers containing a  $\beta$ -sheet structure, as Ishii and coworkers suggested [24, 25].

**3.2. Secondary Structure of E22 $\Delta$  Mutants.** To investigate the secondary structure of E22 $\Delta$ -A $\beta$ 40 and E22 $\Delta$ -A $\beta$ 42, their CD spectra were measured. In the control experiment using A $\beta$ 42 (Figure 2(c)), the positive peak at 200 nm and the negative peak at 220 nm gradually increased during the 48-hr incubation, suggesting that transformation of the random organization into a  $\beta$ -sheet structure occurred, while A $\beta$ 40 remained mainly random (Figure 2(a)). In contrast, E22 $\Delta$ -A $\beta$ 42 formed a  $\beta$ -sheet-rich structure immediately after dissolution (Figure 2(d)). The velocity of the transformation of E22 $\Delta$ -A $\beta$ 40 was also higher than that of A $\beta$ 42 (Figure 2(b)).

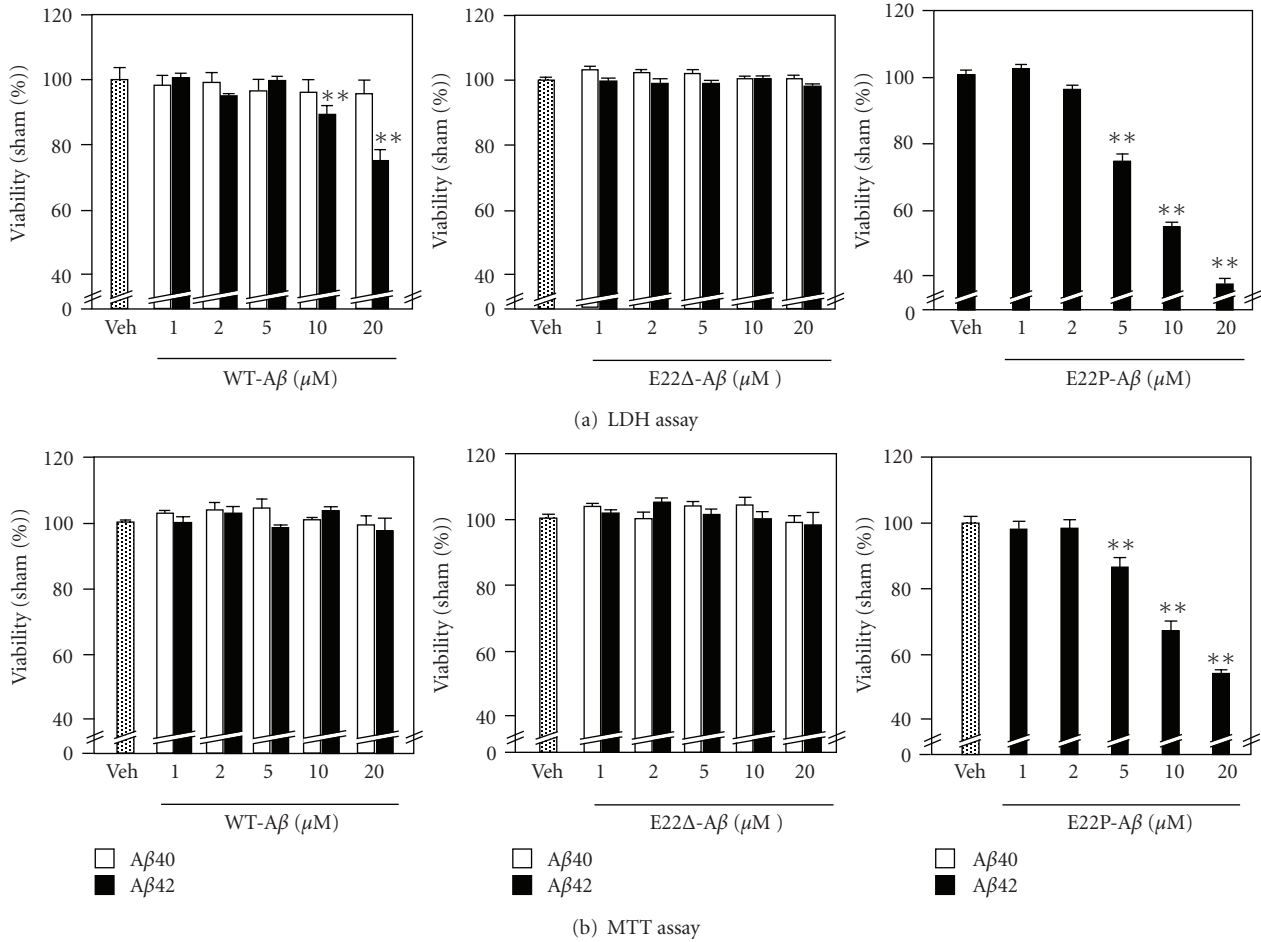


FIGURE 4: Neurotoxicity of Aβ40, Aβ42, E22Δ-Aβ40, E22Δ-Aβ42, and E22P-Aβ42 with the indicated concentration (1, 2, 5, 10, and 20 μM) using primary rat cortical neuronal cell cultures after 48-hr incubation at 37°C. Data are expressed as the mean ± s.e.m. \*P < .05 versus vehicle, \*\*P < .01 versus vehicle. Veh: vehicle.

These results suggest that the E22Δ mutation induces β-sheet transformation to form Aβ oligomers under our condition.

3.3. *Radical Production by E22Δ Mutants.* Our previous studies suggested that the radical productivity of Aβ42 mutants at position 22 such as E22P-, E22K-, E22Q-, and E22G-Aβ42 correlated with their aggregative ability and neurotoxicity [7]. To investigate the effect of E22Δ mutation in Aβs on the radical-generating activity, ESR was measured using phenyl-*N-tert*-butylnitron (PBN) as a spin-trapping reagent (Figure 3). ESR signals of E22Δ-Aβ40 were twice more potent than those of Aβ40, and E22Δ-Aβ42 also showed slightly stronger signals than Aβ42. The radical productivity of the E22Δ-Aβs correlated basically with their ability to form oligomers and a β-sheet structure (Figures 1(c), 2).

3.4. *Neurotoxicity of E22Δ-Aβs in Primary Rat Cortical Neuronal Cell Cultures.* Having demonstrated that E22Δ mutation enhanced the β-sheet structure and radical productivity, we assessed the effect of this mutation on the

neurotoxicity in primary rat cortical neuronal cell cultures by LDH and MTT assay (Figure 4). Treatment of the neurons with 1–20 μM of wild-type Aβ42 for 2 days induced neurotoxicity in a dose-dependent manner in the LDH test (Figure 4(a), left), in which the released LDH of the damaged cells (mainly neurons) was measured in the medium. E22P-Aβ42 with a turn at positions 22, and 23 induced stronger damage to the neurons than wild-type Aβ42; cell viability was less 40% at 20 μM (Figure 4(a), right). On the other hand, the difference in cell viability between the vehicle and wild-type Aβ42 did not reach a significant level in the MTT assay even at 20 μM (Figure 4(b), left). The cell viability of E22P-Aβ42 in MTT was also about 50% at 20 μM. In the MTT assay, total cells containing neurons, astrocytes, and microglia damaged by Aβs were counted. Since the neurons are more sensitive to damage than astrocytes or microglia in the primary cell cultures [26], the “neurotoxicity” estimated by the LDH test is often stronger than that evaluated by the MTT test.

It is worth noting that E22Δ-Aβ40 and E22Δ-Aβ42 as well as Aβ40 at 20 μM failed to show neurotoxicity against the primary cultures both in the LDH and MTT tests (Figure 4). These results are consistent with those reported by Takuma

et al.; the neurotoxicity of E22 $\Delta$ -A $\beta$ 42 was very weak against mouse neuroblastoma Neuro-2a and human neuroblastoma IMR-32 [15]. In our MTT test using rat neuroblastoma PC12 cells, the IC<sub>50</sub> of E22 $\Delta$ -A $\beta$ 42 and wild-type A $\beta$ 42 was  $4.6 \pm 1.1 \mu\text{M}$  and  $0.65 \pm 0.11 \mu\text{M}$ , respectively, showing that E22 $\Delta$ -A $\beta$ 42 was significantly less toxic than wild-type A $\beta$ 42. The neurotoxicity of E22 $\Delta$ -A $\beta$ 40 (IC<sub>50</sub> =  $10 \pm 1.0 \mu\text{M}$ ) was weak as expected, but slightly stronger than that of A $\beta$ 40 (IC<sub>50</sub> =  $20 \pm 1.0 \mu\text{M}$ ).

**3.5. Synaptotoxicity of E22 $\Delta$  Mutants.** Selkoe and coworkers suggested that A $\beta$  dimers are the smallest synaptotoxic species inhibiting the LTP in the pathogenesis of AD and that plaque cores are largely inactive but sequester and release dimers [27]. Tomiyama et al. reported the more potent inhibition of LTP by E22 $\Delta$ -A $\beta$ 42 than by wild-type A $\beta$ 42 [14]. We tested the inhibition of LTP by E22 $\Delta$ -A $\beta$ 40 using rat hippocampal slices. Figure 5 shows that E22 $\Delta$ -A $\beta$ 40 is not such a potent inhibitor of LTP as E22 $\Delta$ -A $\beta$ 42, whose inhibitory potency was stronger than that of wild-type A $\beta$ 42, as Tomiyama et al. reported [14]. This coincides with the previous data that the 42-mer A $\beta$  showed more potent neurotoxicity than 40-mer A $\beta$  [13]. Notably, E22P-A $\beta$ 42, which can more readily form a toxic conformer with a turn at positions 22 and 23 than wild-type A $\beta$ 42 [11], inhibited the LTP more strongly than E22 $\Delta$ -A $\beta$ 42 at an almost undetectable level after 60 min (Figure 5(b)). This suggests that the conformation at positions 22 and 23 of E22P-A $\beta$ 42 might be similar to that of E22 $\Delta$ -A $\beta$ 42 at positions 21 and 23.

**3.6. Relevance of E22 $\Delta$  Mutation to Turn-Induced Neurotoxicity.** The present results suggest that E22 $\Delta$  mutation in A $\beta$  accelerates the transformation of a random form into a  $\beta$ -sheet structure (Figure 2) and radical productivity (Figure 3) but does not increase neurotoxicity in primary rat cortical neuronal cell cultures (Figure 4). E22 $\Delta$ -A $\beta$ 42 synthesized in our laboratory showed the significant formation of oligomers (Figure 1) and synaptotoxicity (Figure 5), as reported by Mori and coworkers [14]. In addition, E22P-A $\beta$ 42 inhibited LTP more severely than E22 $\Delta$ -A $\beta$ 42 (Figure 5). We previously reported that E22P-A $\beta$ 42, with a turn at positions 22 and 23 as a Pro-X corner (X: variable amino acid residue) [28], could form significant oligomers [11] with a  $\beta$ -sheet-rich structure [16] and radicals to result in potent neurotoxicity with the formation of radicals [7]; therefore, E22 $\Delta$ -induced synaptotoxicity might be in part related to turn-induced radical formation. This implies that conformational change in E22 $\Delta$ -A $\beta$  is similar to that in E22P-A $\beta$ 42, but is not the same since E22 $\Delta$ -A $\beta$ 42 exhibited no neurotoxicity, unlike E22P-A $\beta$ 42 and wild-type A $\beta$ 42.

It should be noted that the effects of E22 $\Delta$  mutation on the physicochemical properties of A $\beta$ 40 are significantly higher than those of A $\beta$ 42. This tendency is similar to cases of other CAA or FAD mutant A $\beta$ s. We previously reported a comprehensive study on the aggregation, neurotoxicity, and secondary structure of A $\beta$  mutants at positions 21–23 (A21G, E22G, E22Q, E22K, and D23N) [13]. Since A $\beta$ 40

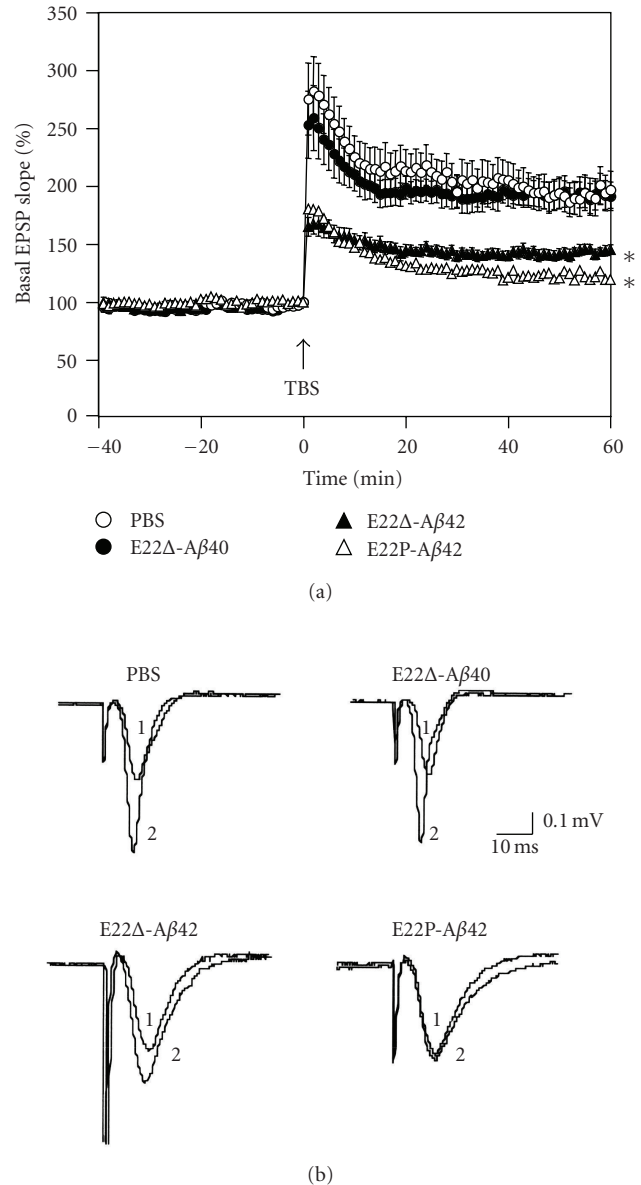


FIGURE 5: *In vivo* synaptotoxicity of E22 $\Delta$ -A $\beta$ 40, E22 $\Delta$ -A $\beta$ 42, and E22P-A $\beta$ 42 estimated by LTP expression. (a) Field excitatory postsynaptic potentials (fEPSPs) were recorded from the CA1 region of rat hippocampal slices (Wistar rats, male, 6 weeks old) by delivering theta burst stimulation (TBS) to the Schaffer collateral/commissural pathway. LTP was induced by high-frequency stimulation (5 trains consisted of four 100-Hz pulses with an intertrain interval of 200 ms) in the presence and absence of each A $\beta$  ( $20 \mu\text{g}/200 \text{ mL}$  PBS), to be injected into the lateral ventricle 20 min before stimulation. Each point on the graph represents the mean  $\pm$  s.e.m. of basal fEPSP slope (0 min);  $n = 12$  for PBS,  $n = 9$  for E22 $\Delta$ -A $\beta$ 40,  $n = 10$  for E22 $\Delta$ -A $\beta$ 42, and  $n = 10$  for E22P-A $\beta$ 40. \*  $P < .0001$  versus PBS;  $P = .4258$  between PBS and E22 $\Delta$ -A $\beta$ 40.  $P < .0001$  versus PBS, when fEPSP slopes were compared with 1 to 60 min after TBS. The means between the four groups were compared using analysis of variance followed by Fisher's protected least significant difference (PLSD) test.  $\circ$ , PBS;  $\bullet$ , E22 $\Delta$ -A $\beta$ 40;  $\blacktriangle$ , E22 $\Delta$ -A $\beta$ 42;  $\triangle$ , E22P-A $\beta$ 42. (b) Typical field excitatory postsynaptic potentials at (1) 0 and (2) 60 minutes after TBS.

is secreted in neurons about nine times more abundantly than A $\beta$ 42 [3], in some cases A $\beta$ 40 may play a critical role in the pathogenesis of CAA or FAD. In addition, the E22 $\Delta$  mutant of A $\beta$ 40 [14] as well as the CAA- or FAD-related A $\beta$ 40 mutants at positions 21, 22, and 23 have been reported to be more resistant than wild-type A $\beta$ 40 against degradation by insulin-degrading enzyme [29]; however, it remains controversial whether E22 $\Delta$  is a familial type of AD or AD-type dementia.

Mori, Tomiyama, and coworkers implied the intracellular accumulation of A $\beta$  oligomers using cultured cells [30] and their own developed mouse model [31] with E22 $\Delta$  mutation. This mutation also caused apoptosis induced by stress in the endoplasmic reticulum [30]. Quite recently, we proposed the involvement of a turn at positions 22 and 23 of A $\beta$  in intracellular amyloidosis [32]. Thus, the increase of radical productivity by E22 $\Delta$  mutation is in good agreement with the turn-induced oxidative stress of A $\beta$ 42 [7], presumably *via* the interplay between Tyr10 and Met35 [12]. The deletion mutation of the residue at position 22 might promote Tyr10 in close proximity to the sulfur atom of Met35, inducing the effective production of radicals.

#### 4. Conclusion

In summary, E22 $\Delta$ -A $\beta$ 42 effectively induced the transformation of a random form to a  $\beta$ -sheet structure and the formation of radicals accompanied with oligomerization. However, the molecular mechanism of the pathology of AD of E22 $\Delta$ -A $\beta$ 42 might be different from that of wild-type A $\beta$ 42 since E22 $\Delta$ -A $\beta$ 42 showed more potent synaptotoxicity but weaker neurotoxicity than wild-type A $\beta$ 42.

#### Acknowledgments

The authors thank Dr. Hiroyuki Fukuda at the Institute of Medical Science, The University of Tokyo for MALDI-TOF-MS measurements, and Drs. Noriaki Kinoshita and Yuko Horikoshi-Sakuraba at Immuno-Biological Laboratories Co., Ltd. for providing the antibody 82E1. This research was supported in part by grants-in-aid for Scientific Research (A) (Grant no. 21248015 to K.I.) and Scientific Research (C) (Grant no. 22603006 to K.M.) from the Ministry of Education, Culture, Sports, Science and Technology of the Japanese Government and in part by the Alzheimer's Association (IIRG-09-132098) to HM.

#### References

- [1] G. G. Glenner and C. W. Wong, "Alzheimer's disease: initial report of the purification and characterization of a novel cerebrovascular amyloid protein," *Biochemical and Biophysical Research Communications*, vol. 120, no. 3, pp. 885–890, 1984.
- [2] C. L. Masters, G. Simms, and N. A. Weinman, "Amyloid plaque core protein in Alzheimer disease and Down syndrome," *Proceedings of the National Academy of Sciences of the United States of America*, vol. 82, no. 12, pp. 4245–4249, 1985.
- [3] C. Haass and D. J. Selkoe, "Soluble protein oligomers in neurodegeneration: lessons from the Alzheimer's amyloid  $\beta$ -peptide," *Nature Reviews Molecular Cell Biology*, vol. 8, no. 2, pp. 101–112, 2007.
- [4] C. Behl, J. B. Davis, R. Lesley, and D. Schubert, "Hydrogen peroxide mediates amyloid  $\beta$  protein toxicity," *Cell*, vol. 77, no. 6, pp. 817–827, 1994.
- [5] D. A. Butterfield, "Amyloid  $\beta$ -peptide [1–42]-associated free radical-induced oxidative stress and neurodegeneration in Alzheimer's disease brain: mechanisms and consequences," *Current Medicinal Chemistry*, vol. 10, no. 24, pp. 2651–2659, 2003.
- [6] K. J. Barnham, C. L. Masters, and A. I. Bush, "Neurodegenerative diseases and oxidatives stress," *Nature Reviews Drug Discovery*, vol. 3, no. 3, pp. 205–214, 2004.
- [7] K. Murakami, K. Irie, H. Ohigashi et al., "Formation and stabilization model of the 42-mer A $\beta$  radical: implications for the long-lasting oxidative stress in Alzheimer's disease," *Journal of the American Chemical Society*, vol. 127, no. 43, pp. 15168–15174, 2005.
- [8] K. Murakami, Y. Masuda, T. Shirasawa, T. Shimizu, and K. Irie, "The turn formation at positions 22 and 23 in the 42-mer amyloid  $\beta$  peptide: the emerging role in the pathogenesis of Alzheimer's disease," *Geriatrics and Gerontology International*, vol. 10, supplement 1, pp. S169–S179, 2010.
- [9] D. M. Walsh, I. Klyubin, J. V. Fadeeva et al., "Naturally secreted oligomers of amyloid  $\beta$  protein potently inhibit hippocampal long-term potentiation in vivo," *Nature*, vol. 416, no. 6880, pp. 535–539, 2002.
- [10] R. Roychaudhuri, M. Yang, M. M. Hoshi, and D. B. Teplow, "Amyloid  $\beta$ -protein assembly and Alzheimer disease," *Journal of Biological Chemistry*, vol. 284, no. 8, pp. 4749–4753, 2009.
- [11] Y. Masuda, S. Uemura, R. Ohashi et al., "Identification of physiological and toxic conformations in A $\beta$ 42 aggregates," *ChemBioChem*, vol. 10, no. 2, pp. 287–295, 2009.
- [12] K. Murakami, H. Hara, Y. Masuda, H. Ohigashi, and K. Irie, "Distance measurement between Tyr10 and Met35 in amyloid beta by site-directed spin-labeling ESR spectroscopy: implications for the stronger neurotoxicity of A $\beta$ 42 than A $\beta$ 40," *Chembiochem*, vol. 8, no. 18, pp. 2308–2314, 2007.
- [13] K. Murakami, K. Irie, A. Morimoto et al., "Neurotoxicity and physicochemical properties of A $\beta$  mutant peptides from cerebral amyloid angiopathy: implication for the pathogenesis of cerebral amyloid angiopathy and Alzheimer's disease," *Journal of Biological Chemistry*, vol. 278, no. 46, pp. 46179–46187, 2003.
- [14] T. Tomiyama, T. Nagata, H. Shimada et al., "A new amyloid  $\beta$  variant favoring oligomerization in Alzheimer's-type dementia," *Annals of Neurology*, vol. 63, no. 3, pp. 377–387, 2008.
- [15] H. Takuma, R. Teraoka, H. Mori, and T. Tomiyama, "Amyloid- $\beta$  E22 $\Delta$  variant induces synaptic alteration in mouse hippocampal slices," *NeuroReport*, vol. 19, no. 6, pp. 615–619, 2008.
- [16] K. Murakami, K. Irie, A. Morimoto et al., "Synthesis, aggregation, neurotoxicity, and secondary structure of various A $\beta$ 1–42 mutants of familial Alzheimer's disease at positions 21–23," *Biochemical and Biophysical Research Communications*, vol. 294, no. 1, pp. 5–10, 2002.
- [17] H. Naiki and F. Gejyo, "Kinetic analysis of amyloid fibril formation," *Methods in Enzymology*, vol. 309, pp. 305–318, 1999.
- [18] S. Varadarajan, J. Kanski, M. Aksenova, C. Lauderback, and D. A. Butterfield, "Different mechanisms of oxidative stress and neurotoxicity for Alzheimer's A $\beta$ (1–42) and A $\beta$ (25–35),"

- Journal of the American Chemical Society*, vol. 123, no. 24, pp. 5625–5631, 2001.
- [19] K. Murakami, M. Uno, Y. Masuda, T. Shimizu, T. Shirasawa, and K. Irie, "Isomerization and/or racemization at Asp23 of A $\beta$ 42 do not increase its aggregative ability, neurotoxicity, and radical productivity in vitro," *Biochemical and Biophysical Research Communications*, vol. 366, no. 3, pp. 745–751, 2008.
- [20] M. S. Shearman, C. I. Ragan, and L. L. Iversen, "Inhibition of PC12 cell redox activity is a specific, early indicator of the mechanism of  $\beta$ -amyloid-mediated cell death," *Proceedings of the National Academy of Sciences of the United States of America*, vol. 91, no. 4, pp. 1470–1474, 1994.
- [21] T. Kume, H. Kouchiyama, S. Kaneko et al., "BDNF prevents NO mediated glutamate cytotoxicity in cultured cortical neurons," *Brain Research*, vol. 756, no. 1-2, pp. 200–204, 1997.
- [22] T. Kume, H. Nishikawa, H. Tomioka et al., "p75-mediated neuroprotection by NGF against glutamate cytotoxicity in cortical cultures," *Brain Research*, vol. 852, no. 2, pp. 279–289, 2000.
- [23] T. Nishizaki, T. Nomura, T. Matuoka et al., "The anti-dementia drug nefiracetam facilitates hippocampal synaptic transmission by functionally targeting presynaptic nicotinic ACh receptors," *Molecular Brain Research*, vol. 80, no. 1, pp. 53–62, 2000.
- [24] S. Chimon and Y. Ishii, "Capturing intermediate structures of Alzheimer's  $\beta$ -amyloid, A $\beta$ (1–40), by solid-state NMR spectroscopy," *Journal of the American Chemical Society*, vol. 127, no. 39, pp. 13472–13473, 2005.
- [25] S. Chimon, M. A. Shaibat, C. R. Jones, D. C. Calero, B. Aizezi, and Y. Ishii, "Evidence of fibril-like  $\beta$ -sheet structures in a neurotoxic amyloid intermediate of Alzheimer's  $\beta$ -amyloid," *Nature Structural and Molecular Biology*, vol. 14, no. 12, pp. 1157–1164, 2007.
- [26] M. R. Vargas and J. A. Johnson, "The Nrf2-ARE cytoprotective pathway in astrocytes," *Expert reviews in molecular medicine*, vol. 11, p. e17, 2009.
- [27] G. M. Shankar, S. Li, T. H. Mehta et al., "Amyloid- $\beta$  protein dimers isolated directly from Alzheimer's brains impair synaptic plasticity and memory," *Nature Medicine*, vol. 14, no. 8, pp. 837–842, 2008.
- [28] P. Y. Chou and G. D. Fasman, " $\beta$ -Turns in proteins," *Journal of Molecular Biology*, vol. 115, no. 2, pp. 135–175, 1977.
- [29] L. Morelli, R. Llovera, S. A. Gonzalez et al., "Differential degradation of amyloid  $\beta$  genetic variants associated with hereditary dementia or stroke by insulin-degrading enzyme," *Journal of Biological Chemistry*, vol. 278, no. 26, pp. 23221–23226, 2003.
- [30] K. Nishitsuji, T. Tomiyama, K. Ishibashi et al., "The E693 $\Delta$  mutation in amyloid precursor protein increases intracellular accumulation of amyloid  $\beta$  oligomers and causes endoplasmic reticulum stress-induced apoptosis in cultured cells," *American Journal of Pathology*, vol. 174, no. 3, pp. 957–969, 2009.
- [31] T. Tomiyama, S. Matsuyama, H. Iso et al., "A mouse model of amyloid  $\beta$  oligomers: their contribution to synaptic alteration, abnormal tau phosphorylation, glial activation, and neuronal loss in vivo," *Journal of Neuroscience*, vol. 30, no. 14, pp. 4845–4856, 2010.
- [32] K. Murakami, Y. Horikoshi-Sakuraba, N. Murata et al., "Monoclonal antibody against the turn of the 42-residue amyloid beta protein at positions 22 and 23," *ACS Chemical Neuroscience*, vol. 1, no. 11, pp. 747–756, 2010.